

Lab on a Chip

Accepted Manuscript



This is an *Accepted Manuscript*, which has been through the Royal Society of Chemistry peer review process and has been accepted for publication.

Accepted Manuscripts are published online shortly after acceptance, before technical editing, formatting and proof reading. Using this free service, authors can make their results available to the community, in citable form, before we publish the edited article. We will replace this *Accepted Manuscript* with the edited and formatted *Advance Article* as soon as it is available.

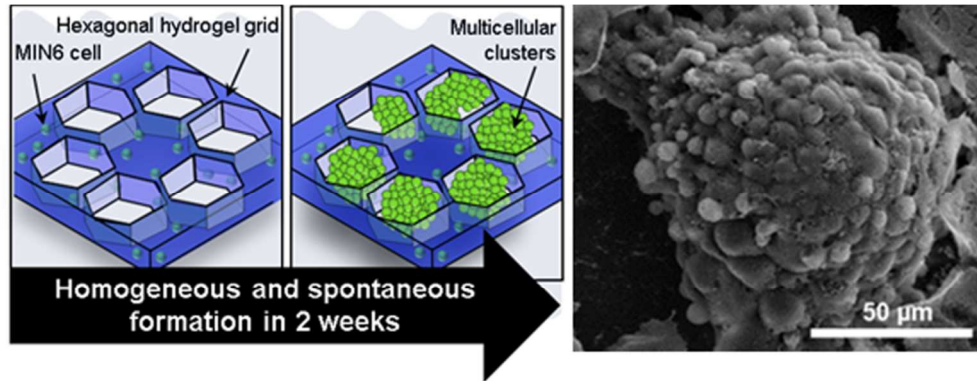
You can find more information about *Accepted Manuscripts* in the [Information for Authors](#).

Please note that technical editing may introduce minor changes to the text and/or graphics, which may alter content. The journal's standard [Terms & Conditions](#) and the [Ethical guidelines](#) still apply. In no event shall the Royal Society of Chemistry be held responsible for any errors or omissions in this *Accepted Manuscript* or any consequences arising from the use of any information it contains.

Geometric effect of the hydrogel grid structure on in vitro formation of homogeneous MIN6 cell clusters

Chae Yun Bae, Mun-kyeong Min, Hail Kim* and Je-Kyun Park*

Floating hydrogel–cell membrane constructs with hexagonal grid structure are exploited for spontaneous formation of homogeneous MIN6 cell clustering, which can be used as pancreatic pseudo-islets enhancing insulin secretion.



ARTICLE

Geometric effect of the hydrogel grid structure on in vitro formation of homogeneous MIN6 cell clusters

Cite this: DOI: 10.1039/x0xx00000x

Chae Yun Bae,^a Mun-kyeong Min,^b Hail Kim^{*b} and Je-Kyun Park^{*a}Received 00th January 2012,
Accepted 00th January 2012

DOI: 10.1039/x0xx00000x

www.rsc.org/

A microstructure-based hydrogel was employed to study the relationship between spatial specificity and cellular behavior, including cell fate, proliferation, morphology, and insulin secretion in pancreatic β -cells. To effectively form homogeneous cell clusters in vitro, we made cell-containing hydrogel membrane constructs with an adapted grid structure based on a hexagonal micropattern. Homogeneous cell clusters (average diameter: $83.6 \pm 14.2 \mu\text{m}$) of pancreatic insulinoma, MIN6 cell, were spontaneously generated in the floating hydrogel membrane constructs, including a hexagonal grid structure (size of cavity: $100 \mu\text{m}$, intervals between cavities: $30 \mu\text{m}$). Interestingly, 3D clustering of MIN6 cells mimicking the structure of pancreatic islets was coalesced into a merged aggregate attaching to the each hexagonal cavity of the hydrogel grid structure. The fate and insulin secretion of homogeneous cell clusters in the hydrogel grid structure were also assessed. The results of these designable hydrogel–cell membrane constructs suggest that facultative in vitro β -cell proliferation and maintenance can be applied to biofunctional assessments.

Introduction

Hydrogels have been widely used as scaffolds to support structural integrity¹ for stem cell differentiation² or cell aggregation,³ and to encapsulate or deliver cells for tissue engineering⁴ and transplantation.⁵ However, enhancement of cellular behavior and proliferation was restricted via the modification of hydrogel conjugation^{3,6,7} or the addition of extracellular matrix (ECM) such as gelatin² and collagen.⁵ Even though the modification of hydrogel conjugation or the addition of ECM was known to improve the cellular function to facilitate cell–ECM interaction or to adjust pore sizes of hydrogel, a geometric control of hydrogel constructs could also be essential to understand cellular growth or function for effective cell–cell contacts and complicated tissue reconstruction of a defined geometry of the limit set.

The use of micro-scale technology has recently increased and has provided further insight into the relationship between physicochemical properties and biological cell behavior. Above all, the geometric control of surrounding microenvironment in cells and tissues is widely recognized to be a critical regulator for understanding the transient role in cell proliferation and multicellular generation for tissue reconstruction with relevance to the regulation of fate,^{7,8} differentiation^{9–11} and morphogenesis.^{12–14} However, a micro-scaled geometric control of hydrogel constructs surrounding cells was extremely complicated because of fabrication process.^{6,15,16} Encapsulated cells were immensely influenced by not only pore sizes of hydrogel but also the surrounding geometry of the scaffold due to difference of mechanical stress and limitation of diffusion length. Therefore, well-designed geometric condition of

hydrogel constructs would stand a better chance of enhancing cell proliferation and multicellular generation for tissue reconstruction without any conjugational modification or additional ECM in hydrogel.

Insulin-producing pancreatic β -cells are typically formed with other endocrine cells in a spherical multicellular group, called the islet of Langerhans, which grows to approximately $100\text{--}200 \mu\text{m}$ in diameter in most species. When they were dissociated into single cells, however, their function was reduced. A similar phenomenon has also been shown for pancreatic insulinoma (MIN6) cells.^{17,18} Although some conventional aggregation techniques, such as simple shaking¹⁹ and hanging drop,²⁰ have been demonstrated for generation of multicellular units, physical size was could hardly be controllable. An array of micro-sized-well structure was used to rapidly achieve homogeneity of generated aggregation.^{5,21} Nevertheless, necrosis of aggregated cells would be usually observed at the center of the bigger clusters within a few days when multicellular clusters were generated. Although it was suggested that various methods can be used to suddenly adhere among cells or attach each other, it was not verifiable to naturally develop a cellular cluster. To implement an in-depth research of cellular growth and maintenance in vitro for longer period of time, we need to spontaneously generate cellular clusters with their own capability, controlling surrounded environmental factors such as physical confinement and chemical elements.

In this paper, we modified previously reported facile fabrication method of mesoscopic free-standing hydrogel structure^{22,23} to construct in vivo-like 3D cellular clusters with particular surrounding microenvironment geometry. To demonstrate a geometric effect of hydrogel constructs in cell

proliferation and maintenance, MIN6 cells were examined for multi-cellular clustering in geometrically confined hydrogel scaffold without any material modification. Here, we suggested a cell-embedded hydrogel membrane constructs, including a hexagonal grid structure with a certain type of micropattern, in consideration of chemical diffusion and cellular interactions. Homogeneous MIN6 cell clusters were generated spontaneously at the cavities of the hexagonal grid structure during 15 culture days. Furthermore, multicellular clusters, generated from the membrane-based floating hydrogel constructs including a hexagonal grid structure, were assessed as their viability and insulin secretion.

Experimental

Preparation of hydrogel microstructure

Free-standing micropatterned hydrogel constructs were fabricated by previously reported method^{22,23} with some modifications. To construct uniform hexagonal grid structure, a poly(dimethylsiloxane)(PDMS) replica was fabricated via two-step lithography. Then, the PDMS replica molds were sterilized overnight by germicidal ultraviolet irradiation on a clean bench. Sodium alginate precursor (1% (w/v); from brown algae, Sigma-Aldrich, St. Louis, MO) in phosphate-buffered saline (PBS; Gibco/Life Technologies, Carlsbad, CA) and 100 mM calcium chloride dehydrate ($\text{CaCl}_2 \cdot 2\text{H}_2\text{O}$; Sigma-Aldrich) in distilled water were used as the ionically cross-linkable hydrogel and cross-linking reagents. Both the sodium alginate precursor and calcium chloride were pre-filtered through a 0.22- μm pore sized filter (Millipore, Billerica, MA). After the plasma treatment of PDMS substrate to create a hydrophilic surface, the hydrogel mixture with single-dispersed cells was coated on the hexagonal pillar structure of the PDMS mold. A controlled volume (7–10 μL) of hydrogel precursors in a MIN6 cell suspension (cell seeding density: 1×10^6 – 10×10^6 cells/mL) was introduced as a thin film (50–70 μm thick) via pipette. The thin film of hydrogel precursor was then cross-linked with a nebulized aerosol of gelling reagent, calcium chloride, within 5 min using a nebulizer with an ultrasonic transducer (fuming rate: 20 mL/min) to develop a smooth surface of the hydrogel construct. The hydrogel constructs were then submerged in cell culture medium and released from the substrate as a floating membrane construct. Each hydrogel construct was incubated with culture media (Dulbecco's modified Eagle's medium with 4.5 g/L glucose supplemented with 15% fetal bovine serum, 100 mg/L penicillin-streptomycin and 71.5 μM 2-mercaptoethanol) for two weeks.

Morphological analysis of fluorescence-stained cell clusters

To analyze morphological characteristics of cellular clusters, floating hydrogel membrane constructs including MIN6 clusters were stained with 10 μM CellTracker™ green CMFDA (Invitrogen, OR). The average diameter and roundness of each stained MIN6 cell clusters were fitted to an ellipse and analyzed by adjusting images using the particle analyzing method of the ImageJ software (<http://rsbweb.nih.gov>). To qualitatively examine z-stacked live cell images, live/dead-stained MIN6 cell clusters attaching to the hexagonal hydrogel grid structure were visualized by confocal microscopy. Encapsulated or adhered cells were stained with 10 μM calcein AM and 4 μM ethidium homodimer-1 (red) for 30 min. A 3D image was reconstructed from each sequential confocal slice (z-axis interval = 10 μm) via ImageSurfer (<http://imagesurfer.cs.unc.edu>).

Scanning electron microscopy (SEM)

The cells inside hydrogel grid structure were fixed with 2.5% glutaraldehyde (Sigma-Aldrich) in deionized water for 1 h, and then washed with deionized water. For secondary fixation,⁵ they were immersed in 1% osmium tetroxide (Sigma-Aldrich) in deionized water for 1 h. Fixed cells were subsequently dehydrated in a graded ethanol series (25%, 50%, 75%, 95% and 100%). After dehydration, they were immersed in tetra butyl alcohol (Sigma-Aldrich) for 30 min (three times) at room temperature and frozen at -70 °C. The cells were completely dried using a critical point dryer (Tousimis, MD) to reduce drying shrinkage and mounted on a specimen stub using graphite paste.²⁴ The samples were coated with platinum, and observed under a field-emission scanning electron microscope (Hitachi, Japan).

Cell proliferative assay

Cell proliferation was quantitatively measured using a tetrazolium salt determined metabolic activity (Dojindo, Japan). The metabolic activity of MIN6 cell clusters was measured using a hydrogel membrane construct, without an extra process for harvest and dissociation of cell clusters. Because cell clusters could not be harvested or dissociated during the cultivation period to investigate the effect of the hydrogel grid structure, the metabolic activity of MIN6 cell clusters was continuously analyzed in the hexagonal hydrogel grid structure during a certain period of time. Due to the small number of cells in a hydrogel membrane construct, it was incubated for 4 h chemical reaction, and then the colorimetric result was measured. Color changes were assessed using a microtiter plate reader (SPECTRAMax250; Molecular Devices, Sunnyvale, CA) at 450 nm and normalized to a reference wavelength of 590 nm. It also can provide relative cell number based on the standard linear fit of known serial number of MIN6 cells. Then, cell number of each condition was recalculated by a fitted formula.

Insulin measurement and glucose-stimulated insulin secretion (GSIS) assay

Insulin was measured from collected cell culture media for two weeks. The secreted media and buffer were collected during the floating period in a static culture plate and then frozen at -80 °C. Insulin secretion measurements were performed on days 3, 6, 9 and 12 using a rat/mouse insulin enzyme-linked immunosorbent assay (ELISA) kit (Millipore, MO). A four-parameter algorithm was used to calibrate curve fitting and for data analysis. Each insulin level per cell was measured and calculated using the relative number of cells. GSIS was measured on the basis of a Krebs Ringer bicarbonate (KRB) buffer (130 mM NaCl, 5 mM KCl, 1.25 mM KH_2PO_4 , 1.25 mM MgSO_4 , 2.68 mM CaCl_2 , 5.26 mM NaHCO_3 , and 10 mM HEPES adjusted pH to 7.4) supplemented with 2% bovine serum albumin (BSA) as described previously.²⁵ Each low and high concentration of glucose condition was 2.8 mM and 22.2 mM glucose in KRB buffer. After two weeks of culture, the MIN6 cell clusters were harvested and collected from the hexagonal hydrogel grid structure. However, we do not dissociate cells because GSIS difference was caused by the morphological difference, such as monolayer or cell clusters. The harvested MIN6 cells were preincubated in KRB buffer with 2.8 mM glucose, and then changed with 2.8 mM, 22.2 mM for 30 min. Secreted KRB buffers were sequentially collected and frozen at -80 °C. Then, insulin was also measured by ELISA. GSIS was described as fold change of insulin secretion in high glucose (22.2 mM) buffer to basal insulin level in low glucose (2.8 mM) buffer.

Results and discussion

Fabrication of 3D hexagonal hydrogel grid structure

Figure 1 shows a schematic of hydrogel grid structure with a hexagon-based grid pattern which mimics the size (100–200 μm) of the islets of Langerhans in the pancreas. The hexagonal hydrogel grid structure was successfully constructed on the hexagonal pillar structure of the PDMS mold (Fig. 1A). It can be manipulated within liquid due to the fragility of the biomaterials and a 100- μm -height-membrane type of hydrogel structure suitable for maintaining viable cells. After the cross-linking reaction, cell-embedded hydrogel grid structure, which has a $2.85 \pm 1.49 \mu\text{m}$ -sized pore ($28.9 \pm 1.15\%$ porosity),²⁶ was removed from the PDMS mold (Fig. 1B) and then, the floating hydrogel grid structure was cultured for two weeks (Fig. 1C). During this period, cells were replicated and the aggregated MIN6 cells grew within the empty spaces attaching to the hydrogel structure. The MIN6 cells have merged and coalesced into a group with a specific morphology in contrast with other cell types. A typical epithelial cell, for example, murine pancreatic ductal adenocarcinoma (mPAC) stretched their body following a hexagonal grid pattern in the hydrogel membrane construct, even though both cells are found in the same organ, pancreas.

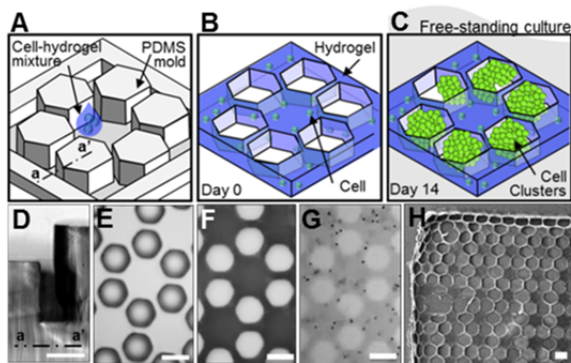


Fig. 1 Schematics of fabrication and images of hexagonal hydrogel grid structure. (A) Schematic of PDMS mold for hexagonal hydrogel grid structure and (B,C) fabricated hexagonal hydrogel grid structure at day 0 and at day 14. (D) Cross-section and (E) top view of the hexagon pillar pattern (height: 150 μm) and guiding frame (height: 100 μm) on PDMS mold with hexagonal grid structures. Hexagonal hydrogel grid structure was stained methylene blue without any particles (F) and (G) with 6- μm polystyrene beads. Hexagonal grid pattern in a hydrogel construct (F,G) has a complete reversal of the PDMS mold (E). (H) The SEM image of hydrogel constructs was also showed hexagonal grid structure. Scale bar = 100 μm .

In our previous work,²³ a monolayer of PDMS replica was prepared to fabricate grid geometries in the hydrogel membrane constructs. This included a scraping process of excessive hydrogel precursors, which might cause a severe damage to the loaded cells. To achieve spatial uniformity of the grid pattern with a simple manner, a PDMS replica was fabricated via two-step lithography (Fig. 1A and 1D). Hydrogel precursor was loaded on the replica mold (Fig. 1A and 1E) that contained a guiding frame (height: 100 μm) and hexagonal pillars for the grid pattern (height: 150 μm) to create an even layer of a hydrogel membrane. Height of the guiding frame was determined from the thickness of hydrogel membrane construct. The hydrogel was stained by methylene blue (3 mg/L) to

visualize optically (Fig. 1F). Instead of cells, monodispersed 6- μm -sized polystyrene beads were demonstrated and were evenly distributed within 3D hydrogel grid structure (Fig. 1G). Both images were totally reversal of hexagonal pillar structures in the PDMS molds. According to a SEM image, the opening parts and precise microstructures of hexagonal hydrogel grid structure were confirmed (Fig. 1H). Using this approach, a more accessible and facile grid microstructure could be constructed without any mechanical stress to the encapsulated cells.

Effect of grid geometry for homogeneous MIN6 cell clustering

To understand the effect of grid geometry as regards nutrient contact on the formation of MIN6 cell clustering, we determined a certain type of design based on an array of hexagons (Fig. 2A). A hexagon is a shape that has densely packed arrangement with uniform intervals for a plane construction as compared with round or other polygons. Although there are lots of geometrical modifications such as a thickness of membrane, a shape of cavity or a repeat of unit pattern, we need only two different factors: the diameter of inner hexagon for cavity (R_i) and the diameter of outer hexagon for hydrogel (R_o). We could generate relatively thin membrane, less than 100 μm , which fully overcomes diffusion depth to accept nutrients into the hydrogel at the vertical direction. Even though cells within hydrogel was sufficiently saturated with the nutrients and oxygen through the upper and bottom side of the hydrogel membrane, a concentration difference of medium could be spatially and temporally occurred at the lateral direction due to a complicated micropattern penetrating a whole plane of hydrogel membrane construct. For example, a close interval between consistent cavities could be favorable for cells to maintain viable and even grow actively in the interior of the hydrogel at the beginning of the culture. Moreover, cells could rapidly grow into a multicellular group at the boundary of cavities, compared to the interior of the hydrogel due to the cross-linked fibers of the hydrogel, which placed so as to be firm cells. However, the excessively dense grid structure could also bring about a weakness of the hydrogel construct and a lack of embedded cells surrounding a cavity. Therefore, biochemical circumstances could be determined in accordance with a combination of various geometric cues in the hydrogel membrane construct.

To geometrically examine the hydrogel membrane construct for generating cell clusters, the size of inner (R_i) and outer (R_o) diameter in the hydrogel grid structure (Fig. 2C, Grid) was determined 100 and 130 μm , respectively, with a certain repeated pattern, in consideration of the circumstances surrounding a cavity, for example, a balance between nutrient diffusion and cell numbers. Total loaded area were equally controlled in a hydrogel membrane without any micropattern (Fig. 2B, None). Otherwise, distances between embedded cells could not be adjusted in hydrogel membrane construct when the equivalent seeding concentration (seeding density: 5×10^6 cells/mL) was constantly applied. Most of cells randomly developed to form an aggregated lump without any pattern in hydrogel membrane construct. On the other hand, cells seem to have a different growth rate in the hexagonal grid pattern depending on the surrounding circumstances, such as medium diffusion, cell-cell distances and surrounding materials. Therefore, MIN6 cell clusters were proliferated into a certain size of lumps and fitted to the cavities in the hexagonal hydrogel grid structure. Although smaller clusters or single cells still remained within the hydrogel grid structure,

homogenous cellular clusters were strongly promoted by geometric controls, occurring in combination of biochemical and physiological environment.

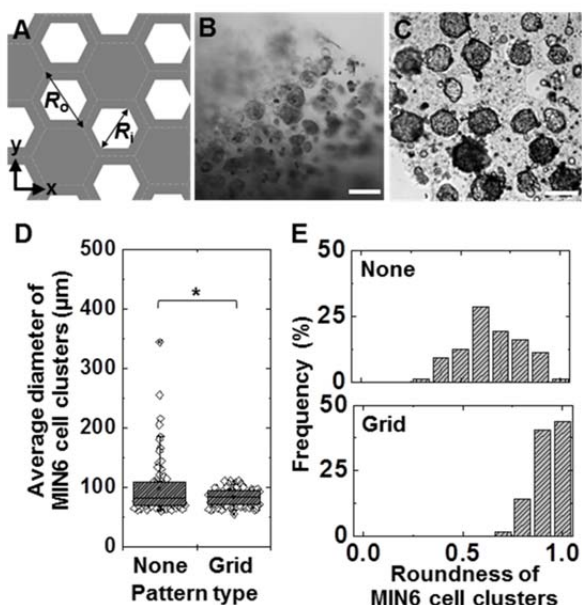


Fig. 2 Schematic and demonstration of a hexagonal hydrogel grid structure. (A) Arrangement of the hexagon pattern has two design factors; a hexagon array of hydrogel (R_o) and a hexagon cavity (R_i). (B–E) Demonstration of hydrogel membrane constructs-based floating cultured MIN6 cells for 13 days without (none, B) or with (grid, C) the hexagonal grid pattern ($R_i = 100 \mu\text{m}$ and $R_o = 130 \mu\text{m}$). (D) Diameters of MIN6 cell clusters in the hydrogel grid structure were significantly different from those in the non-patterned hydrogel constructs (statistical analysis was conducted with one-way ANOVA, $*p < 0.05$, $n = 513$). (E) Roundness of MIN6 cell clusters, the difference between the maximal and minimal widths of cell clusters, were measured to determine morphological homogeneity of cell clusters ($n = 474$). Scale bar = $100 \mu\text{m}$.

Although MIN6 clusters were equally represented by both types of floating membranes as a result of in vitro culture for 13 days, there was a morphologically distinct characteristic of cellular clusters in the hexagonal hydrogel grid structure. The average diameter of MIN6 cell clusters was measured via image analysis of green-fluorescent labeled cellular clusters (Fig. 2D). We selected over a $50\text{-}\mu\text{m}$ -size of clusters to exclude single or non-replicating cells in hydrogel membrane construct. The cell clusters found in the hexagonal hydrogel grid structure were significantly different from those encapsulated within the non-patterned hydrogel structure (The statistical analysis was conducted with one-way ANOVA, $*p < 0.05$, $n = 513$). Each non- and grid pattern yielded cell clusters with average diameters of 97.3 ± 44.5 and $83.6 \pm 14.2 \mu\text{m}$, respectively. Although the average diameter of the MIN6 cell clusters was comparable each other, they were more homogeneous in the hexagonal grid structure than that in non-patterns. In addition, regular round units of cell clusters were more frequently ($> 60\%$ of total units) observed in the hexagonal hydrogel grid structure, when the growing MIN6 cells coalesced into a multi-cellular cluster (Fig. 2E). This implies that multicellular clusters rapidly developed within the geometrically confined hexagon-based grid in the hydrogel membrane construct.

To examine correlation between different sizes of a cavity (R_i), MIN6 cell clusters were generated using hydrogel grid structure, including three different sizes of hexagon cavity unit ($R_i = 100, 150$ and $200 \mu\text{m}$ / $R_o = 130, 195$ and $260 \mu\text{m}$) for 15 days (seeding density: 1×10^7 cells/mL) (Fig. 3). Each condition has an identical ratio of inner size to outer size ($R_i/R_o = 0.77$), which represents an identical design pattern in the hydrogel grid structure. According to the images of cellular clusters at day 15 (Fig. 3A), they had consistent sized-features in common at the same period of cultivation. Each sizes of hydrogel grid structure ($R_i = 100, 150$ and $200 \mu\text{m}$) yielded cell clusters with average diameters of 112.28 ± 23.79 , 112.65 ± 25.67 and $112.55 \pm 25.86 \mu\text{m}$ at day 10, respectively. Their size were generally increased as 116.27 ± 23.05 , 114.55 ± 26.06 and $117.24 \pm 29.70 \mu\text{m}$ at day 15, regardless of pattern size. On the other hand, morphological homogeneity of MIN6 cell clusters was considerably involved in a cavity size due to the confined geometric effect (Fig. 3B). According to the distribution of rounded MIN6 cell clusters, homogeneous rounded clusters were frequently discovered after sufficiently mature cultured at day 15 in $100\text{-}\mu\text{m}$ -sized cavities. Although MIN6 cell clusters could be theoretically raised up in the course of time, however, they would also be large enough to detach from the wall of the hydrogel grid structure. Although this study demonstrates that a slight size variation in the same grid structure does not significantly affect the size of developed clusters, overall the hexagonal micropattern in a grid structure would be involved in homogeneous formation of cellular clusters following confined cavities of the hydrogel grid structure.

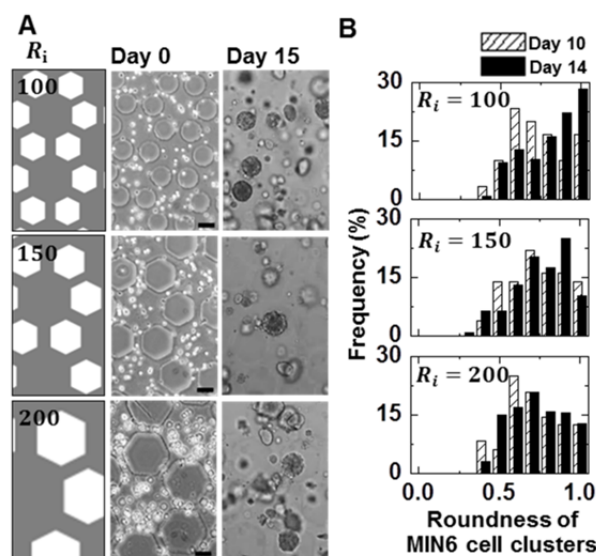


Fig. 3 Effect of hexagonal cavity size in the hydrogel grid structure. (A) MIN6 cell clusters were generated using hydrogel grid structure with different sizes of hexagon pattern ($R_i = 100, 150$ and $200 \mu\text{m}$ / $R_o = 130, 195$ and $260 \mu\text{m}$) for 15 days. (B) Morphological homogeneity of MIN6 cell clusters was measured via image analysis (day 15). Scale bar = $100 \mu\text{m}$.

Most of cavities (over 90% of cavities) were filled with MIN6 cell clusters after the hydrogel membrane construct was floated and cultured for 13 days (Fig. 4A). Closed boundary of MIN6 cell clusters was also identified at the grid cavities in a magnified image (see inset of Fig. 4A). According to the image of a hydrogel grid structure, MIN6 cells not only simply

proliferated into lumps but also assembled into the cavity to effectively generate homogeneous multicellular clusters. This process is a natural and spontaneous method to promote homogeneous multicellular clusters through the micro-scaled geometry of the hydrogel scaffold. To determine details of the clusters attaching to the hydrogel grid structure, we investigated the surface of the hexagonal hydrogel grid structure, including fully formed MIN6 cell clusters via the SEM image (Fig. 4B). Each of MIN6 cell clusters attached to the hydrogel and occupied in a grid cavity; a magnified image showed tight cell-cell contacts with a smooth surface (see inset of Fig. 4B). Moreover, a fully formed MIN6 cluster was raised up to over a 100- μm -sized multicellular cluster, allowing for some shrinkage effects due to the drying process of SEM.

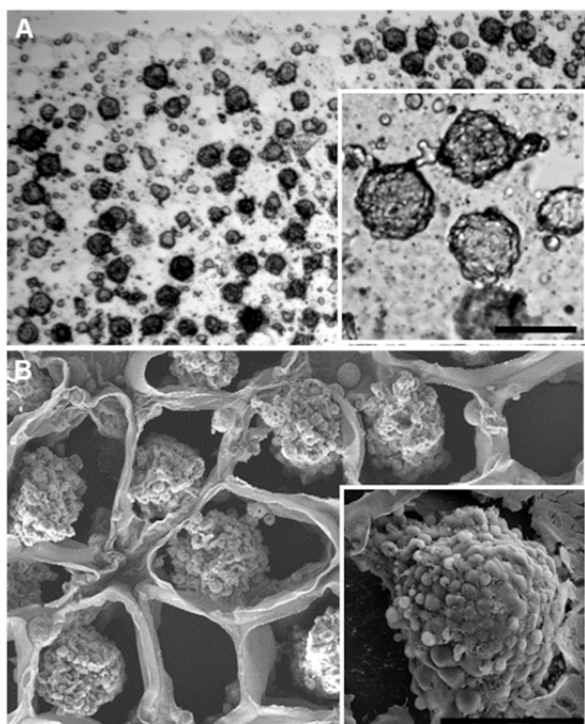


Fig. 4 Distribution of MIN6 cells clustering in the hexagonal hydrogel grid structure. (A) Distribution of MIN6 cell cluster in a single hydrogel membrane construct was optically examined. Homogeneous and frequent aggregation of MIN6 cells was confirmed in an image of a single hydrogel grid structure following hexagonal grid pattern. (B) A magnified SEM image of attached MIN6 clusters to a cavity in the hexagonal grid structure at day 14. Scale bar = 100 μm .

Proliferation of MIN6 cell and viability assessment of MIN6 cell clusters in floating hexagonal hydrogel grid structure

To reveal the generation of MIN6 cell clusters in hexagonal hydrogel grid structure during culture period, cells were observed in a floating hydrogel membrane at day 1, 9 and 13 (Fig. 5A–D). Dispersed single MIN6 cells (5×10^6 cells/mL) were evenly distributed within gelled hydrogels in three dimensions at day 1 (Fig. 5A). Over time, however, cells proliferated and naturally constructed as small size of multicellular clusters within 9 days (Fig. 5B). Very interestingly, over a-week-culture period, cells grew up into a certain size of tight clusters and occupied their positions filling

up each cavity of floating hydrogel membrane construct. Finally, a multicellular cluster has been generated in a certain hexagonal hydrogel grid structure for 14 days (Fig. 5C). Moreover, the cytoplasm was also stained by green fluorescence at day 13 to examine morphology of cellular clusters in stereoscopic view (Fig. 5D). According to the fluorescence image, most of cells placed in the cavities and attached to the hydrogel grid structure, however some of smaller cells or single cell also still existed within the hydrogel membrane construct. Every cell seems to have different proliferative ability because of surrounding circumstances.

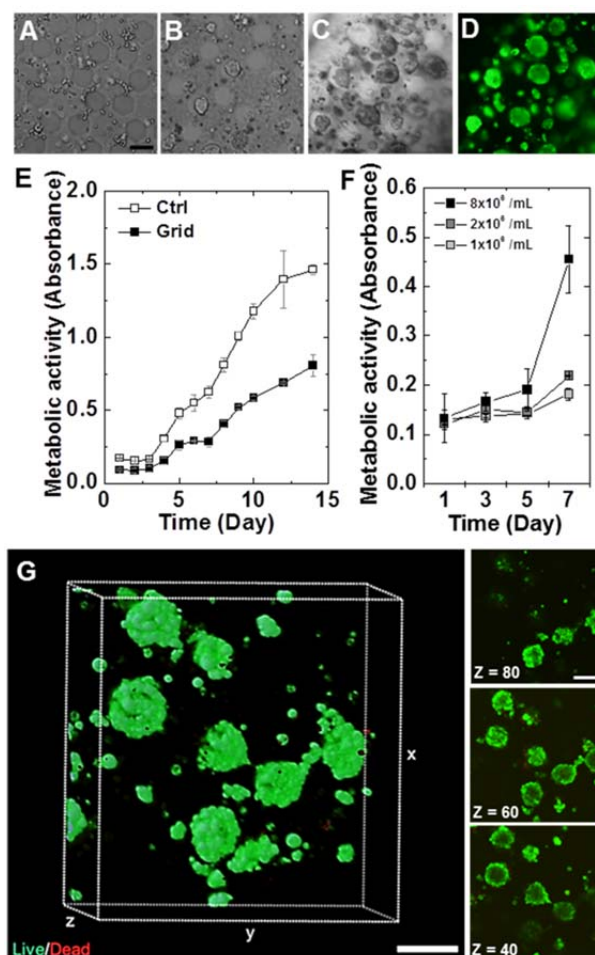


Fig. 5 Viability and insulin producing ability of MIN6 cell clusters within hexagonal hydrogel grid structure. Embedded cells at day 1 (A) proliferated and agglomerated together to form larger clusters in the hexagon cavity at day 9 (B) and day 13 (C). Fluorescence images of CellTracker™ stained cells were obtained on culture day 13 (D). (E,F) Proliferation of MIN6 cells was measured by metabolic activities of cells compared to a 2D conventional dish culture condition (ctrl) for 14 days (E) and with various seeding density in hexagonal hydrogel grid structure (F). (G) Live/dead-stained confocal microscopy images. 3D reconstruction of MIN6 cell clusters after 10 days of floating culture in the hexagonal hydrogel grid structure. Green (calcein-AM): live cell; Red (ethidium homodimer-1): dead cell. Representative images of the six sequential confocal slices ($Z = 40, 60$ and $80 \mu\text{m}$). Scale bar = 100 μm .

To quantitatively measure the growth and proliferation of MIN6 cells in hexagonal hydrogel grid structure, metabolic activity of cells was assessed during the floating culture period of time (Fig. 5E). According to the daily assessment of MIN6

cells, encapsulated MIN6 cells in hexagonal hydrogel grid structure (Grid) were slowly increased compared to the conventional 2D culture condition (Ctrl) (seeding density: 1×10^7 cells/mL). A cellular growth rate in control was universally faster than that in 3D hydrogel condition. However, different cell-seeding density would improve their proliferation in hydrogel condition. It determines the distances between cells and the cell–cell interactions necessary for appropriate cell–cell contact.³ In our condition, grid cavities were also promoting close distances between cells to induce cell–cell interactions during total culture period. However, we also need to find out seeding density would be affect how fast they can grow in the hydrogel grid structure via examining cellular metabolic activity using a tetrazolium salt for a week (Fig. 5F). A cellular growth rate in a conventional 2D culture plate was universally faster than that in 3D hydrogel condition. However, cells rapidly grew and generated into multicellular clusters of the hydrogel grid structure with large number of seeding density (8×10^6 cells/mL). This implies that a large number of encapsulated MIN6 cells will give a synergistic result in generating cell clusters that localize more rapidly to the hexagonal hydrogel grid structure into the certain sizes of cellular units. In addition, relatively small number of cells (1×10^6 cells/mL) would be possible to generate multicellular clusters for longer period of time, over 2 weeks, in contrast with a week-limited conventional culture condition. Consequently, culturing for longer periods likely facilitates to generate MIN6 cell clusters through the encapsulation of the limited number of individual cells.

A 3D image of live/dead-stained MIN6 multicellular clusters was reconstructed to qualitatively analyze cell viability (Fig. 5G) including representative 10 μ m-height series images (see insets of Fig. 5G). After 13 days of floating culture, fully generated cell clusters showed highly viable attaching to the grid cavities and they developed regular distribution patterns following the confined geometry. Few single cells or smaller clusters of which the size was not enough to fill a grid cavity still remained highly viable inside the hydrogel membrane construct. After some of the full-sized cell clusters detached from the hydrogel membrane construct, remaining viable cells could grow and generate another cluster at an adjacent vacancy. Therefore, we could continually obtain size-controlled multicellular clusters in a single hydrogel membrane construct until the embedded cells were exhausted.

Insulin secretion of generated MIN6 cell clusters in floating hexagonal hydrogel grid structure

We also investigated both insulin level and cell number increase for longer period of times in high-glucose media with or without hexagon-grid geometry as regards biochemical effect (Fig. 6A). Metabolic activity was also examined on days 3, 6, 9 and 12 after dispersed MIN6 cells was encapsulated inside hydrogel grid structure. Cell number was normalized to the standard linear fit curve of counted number of MIN6 cells. Based on the cell number, insulin secretion per cell was measured. It was approximately equivalent at the beginning of the culture period; however, as culture progressed, the insulin-secretion level per cell in the hexagon-hydrogel grid structure (Grid) was consistently higher than that in the hydrogel structure without any pattern (None). Moreover, cells at the center of the clusters, necrotic regions, could be damaged at the randomly generated multicellular clusters in the hydrogel structure without any pattern, which reduces the metabolic activity of total cells at day 12. Even though absolute number of

cells was smaller in the hydrogel grid structure, however, both cell number and insulin secretion in the hydrogel grid structure was increasing during a cultivation period. Therefore, the function of MIN6 cells, especially insulin secretion, seems to have high relevance to the regular formation of multicellular clusters through controlling their surrounding geometrical environment.

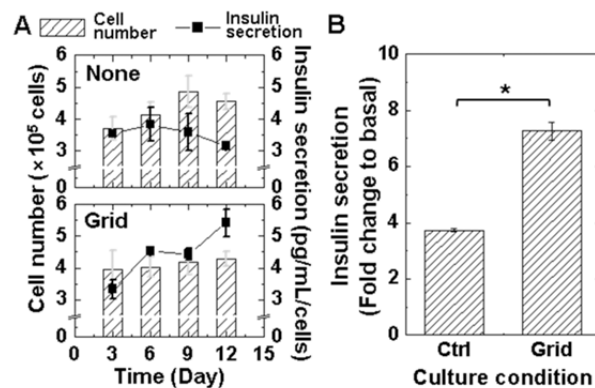


Fig. 6 Insulin secretion of MIN6 cells in the hexagonal hydrogel grid structure. (A) Cell number and accumulated total insulin secretion in high-glucose media was assessed at days 3, 6, 9 and 12 with (grid) or without hexagonal grid pattern (none) in hydrogel membrane constructs. (B) Fold change of glucose-stimulated insulin secretion (GSIS) to basal insulin level was also assessed using generated MIN6 cell clusters in the hexagonal hydrogel grid structure at day 14 compared to a 2D culture condition (Ctrl). Basal insulin level was obtained at low glucose (2.8 mM) KRB buffer and GSIS was obtained at high glucose (22.2 mM) KRB buffer. Larger fold change was related to high sensitivity in glucose response. Statistical significance (student's *t* test) compared to ctrl is indicated: **p* < 0.001, *n* = 3).

To determine the detailed function of MIN6 cell clusters in the hexagonal hydrogel grid structure, GSIS was investigated based on KRB buffer with low glucose (2.8 mM). Fold change was dramatically increased in hexagonal hydrogel grid compared to a 2D condition (Ctrl) when KRB buffer solution containing high glucose (22.2 mM) was applied (Fig 6B, statistical analysis was conducted with student's *t* test, **p* < 0.001, *n* = 3). That is, a multicellular clustered form of MIN6 cells could give a functional benefit compared to the conventional culture condition. Besides, actual insulin level in hexagonal hydrogel grid structure was 0.1774 ± 0.0158 (ng/mL) in low glucose buffer and 1.2846 ± 0.0593 (ng/mL) in high glucose buffer. On the other hand, insulin level in Ctrl was 0.3520 ± 0.0082 (ng/mL) in low glucose buffer (basal) and 3.7331 ± 0.0444 (ng/mL) in high glucose buffer. According to the actual insulin level in both ctrl and hydrogel grid structure, their insulin level was similar to each other at high glucose buffer condition. However, the basal level of secreted insulin from the hexagonal hydrogel grid structure was significantly less than that in Ctrl. When the high concentration of glucose suddenly affected to the MIN6 cells, permeated glucose into the multicellular cluster would be distinguished from reaching to the stretched features in conventional culture dish.

Conclusions

We demonstrated a geometric effect for the formation of homogeneous MIN6 cells clusters via fabrication of

mesoscopic hydrogel grid structure. By examining the morphology, viability and insulin secretion of merged MIN6 cells in a confined cavity of grid structure, certain sizes of cell clusters were homogeneously generated and spontaneously occupied in the hexagonal cavities of the hydrogel membrane constructs during culture. The grid geometry in the hydrogel membrane construct facilitated to generate multicellular clusters with a limited number of seeding densities. The MIN6 cellular clusters were successfully developed without any modification of hydrogel conjugation and additional ECM. Furthermore, GSIS of MIN6 cell clusters in the hexagonal hydrogel grid structure showed a two-fold increase compared with the conventional 2D culture of MIN6 cells. Consequently, facultative in vitro β -cell proliferation and maintenance as a cell clustering form through the geometric control of hydrogel scaffold can be achieved using a hexagon-grid cell-encapsulated hydrogel membrane construct. Therefore, it could be applied not only to transplant of reconstructed tissue but also to the development of biofunctional assays based on modular tissue constructs. Use of appropriate micropatterns may facilitate β -cell culture in vitro, which holds promise for development of an in-depth biofunctional assay for scientific research and development of novel drugs for a variety of metabolic diseases.

Acknowledgements

This research was supported by a National Leading Research Laboratory Program (Grant NRF-2013R1A2A1A05006378) through the National Research Foundation of Korea funded by the Ministry of Science, ICT and Future Planning. The authors also acknowledge a Cooperative Research Program for Agriculture Science and Technology Development (Grant PJ009842) supported by the Rural Development Administration of Korea, and a Korean Health Technology R&D Project (Grant A112024) of the Ministry of Health and Welfare of Korea.

Notes and references

^a Department of Bio and Brain Engineering, Korea Advanced Institute of Science and Technology (KAIST), 291 Daehak-ro, Yuseong-gu, Daejeon 305-701, Republics of Korea. E-mail: jekyun@kaist.ac.kr; Fax: +82-42-350-4310; Tel: +82-42-350-4315.

^b Graduate School of Medical Science and Engineering, Korea Advanced Institute of Science and Technology (KAIST), 291 Daehak-ro, Yuseong-gu, Daejeon 305-701, Republics of Korea. E-mail: hailkim@kaist.edu; Fax: +82-42-350-4243; Tel: +82-42-350-4240.

1. B. V. Slaughter, S. S. Khurshid, O. Z. Fisher, A. Khademhosseini and N. A. Peppas, *Adv. Mater.*, 2009, **21**, 3307-3329.
2. H. Qi, Y. Du, L. Wang, H. Kaji, H. Bae and A. Khademhosseini, *Adv. Mater.*, 2010, **22**, 5276-5281.
3. C.-C. Lin and K. S. Anseth, *Proc. Natl. Acad. Sci. U.S.A.*, 2011, **108**, 6380-6385.
4. Y. T. Matsunaga, Y. Morimoto and S. Takeuchi, *Adv. Mater.*, 2011, **23**, H90-94.
5. B. R. Lee, J. W. Hwang, Y. Y. Choi, S. F. Wong, Y. H. Hwang, D. Y. Lee and S. H. Lee, *Biomaterials*, 2012, **33**, 837-845.
6. A. Sala, P. Hanseler, A. Ranga, M. P. Lutolf, J. Voros, M. Ehrbar and F. E. Weber, *Integr. Biol.*, 2011, **3**, 1102-1111.
7. C. A. DeForest, B. D. Polizzotti and K. S. Anseth, *Nat. Mater.*, 2009, **8**, 659-664.
8. S. Khetan and J. A. Burdick, *Biomaterials*, 2010, **31**, 8228-8234.

9. A. J. Keung, S. Kumar and D. V. Schaffer, *Annu. Rev. Cell Dev. Biol.*, 2010, **26**, 533-556.
10. D. R. Albrecht, G. H. Underhill, T. B. Wassermann, R. L. Sah and S. N. Bhatia, *Nat. Methods*, 2006, **3**, 369-375.
11. A. M. Kloxin, K. J. Lewis, C. A. DeForest, G. Seedorf, M. W. Tibbitt, V. Balasubramaniam and K. S. Anseth, *Integr. Biol.*, 2012, **4**, 1540-1549.
12. C. M. Nelson, M. M. Vanduijn, J. L. Inman, D. A. Fletcher and M. J. Bissell, *Science*, 2006, **314**, 298-300.
13. H. Tekin, J. G. Sanchez, C. Landeros, K. Dubbin, R. Langer and A. Khademhosseini, *Adv. Mater.*, 2012, **24**, 5543-5547, 5542.
14. H. Aubin, J. W. Nichol, C. B. Hutson, H. Bae, A. L. Sieminski, D. M. Cropek, P. Akhyari and A. Khademhosseini, *Biomaterials*, 2010, **31**, 6941-6951.
15. F. Yanagawa, H. Kaji, Y. H. Jang, H. Bae, D. Yanan, J. Fukuda, H. Qi and A. Khademhosseini, *J. Biomed. Mater. Res. A.*, 2011.
16. L. Leng, A. McAllister, B. Zhang, M. Radisic and A. Gunther, *Adv. Mater.*, 2012, **24**, 3650-3658.
17. A. C. Hauge-Evans, P. E. Squires, S. J. Persaud and P. M. Jones, *Diabetes*, 1999, **48**, 1402-1408.
18. M. J. Luther, A. Hauge-Evans, K. L. Souza, A. Jorns, S. Lenzen, S. J. Persaud and P. M. Jones, *Biochem. Biophys. Res. Commun.*, 2006, **343**, 99-104.
19. E. S. O'Sullivan, A. S. Johnson, A. Omer, J. Hollister-Lock, S. Bonner-Weir, C. K. Colton and G. C. Weir, *Diabetologia*, 2010, **53**, 937-945.
20. H. J. Kim, Z. Alam, J. W. Hwang, Y. H. Hwang, M. J. Kim, S. Yoon, Y. Byun and D. Y. Lee, *Transplant. Proc.*, 2013, **45**, 605-610.
21. A. B. Bernard, C.-C. Lin and K. S. Anseth, *Tissue Eng. Part C Methods.*, 2012, **18**, 583-592.
22. W. Lee, J. Son, S.-S. Yoo and J.-K. Park, *Biomacromolecules*, 2011, **12**, 14-18.
23. W. Lee, C. Y. Bae, S. Kwon, J. Son, J. Kim, Y. Jeong, S. S. Yoo and J. K. Park, *Adv. Healthc. Mater.*, 2012, **1**, 635-639.
24. E. Wisse, *World J. Gastroenterol.*, 2010, **16**, 2851.
25. M. Ohara-Imaizumi, H. Kim, M. Yoshida, T. Fujiwara, K. Aoyagi, Y. Toyofuku, Y. Nakamichi, C. Nishiwaki, T. Okamura, T. Uchida, Y. Fujitani, K. Akagawa, M. Kakei, H. Watada, M. S. German and S. Nagamatsu, *Proc. Natl. Acad. Sci. U.S.A.*, 2013, **110**, 19420-19425.
26. S.-h. Kim and C.-C. Chu, *J. Biomed. Mater. Res.*, 2000, **53**, 258-266.